

Deglacial Floods in the Beaufort Sea Preceded Younger Dryas Cooling

L.D. Keigwin^{1*}, S. Klotsko², N. Zhao¹, B. Reilly³, L. Giosan¹, and N.W. Driscoll²

¹Woods Hole Oceanographic Institution, Woods Hole, MA 02543.

²Scripps Institution of Oceanography, UCSD, La Jolla, CA 92093.

³College of Earth, Ocean, and Atmospheric Sciences, OSU, Corvallis, OR 97331.

*Correspondence to: lkeigwin@whoi.edu

The Younger Dryas cooling at ~13 ka, after 2 kyr of postglacial warming, is a century-old climate problem. The Younger Dryas is thought to have resulted from a slow-down of the Atlantic meridional overturning circulation in response to a sudden flood of Laurentide Ice Sheet meltwater that reached the Nordic Seas. Although there is no oxygen isotope evidence in planktonic foraminifera from the open western North Atlantic for a local source of meltwater from the Gulf of St. Lawrence where it was predicted, we report here that the eastern Beaufort Sea contains the long-sought signal of ¹⁸O-depleted water. Beginning at $\sim 12.94 \pm 0.15$ ka, oxygen isotopes in planktonic foraminifera from two sediment cores as well as sediment and seismic data indicate a flood of melt water, ice and sediment to the Arctic via Mackenzie River that lasted about 700 years. The minimum in oxygen isotope ratios lasted ~130 years. The floodwater would have travelled north along the Canadian Archipelago, and through Fram Strait to the Nordic Seas where freshening and freezing near sites of deepwater formation would have suppressed convection, and caused the Younger Dryas cooling by reducing the meridional overturning.

Introduction

It is known that conditions in the Arctic Ocean have a profound effect on the North Atlantic Ocean, for example the Great Salinity Anomaly (GSA) of the 1960s and 1970s¹ and that export of excess fresh water and ice through Fram Strait was the origin of

29 the GSA^{2,3}. During transit of the GSA around convective regions of the Nordic Seas,
30 decreased sea surface salinities and increased sea ice cover reduced convective overturn
31 and contributed to very harsh winters. There is reason to expect that similar and even
32 larger climate events occurred in the past, especially during deglaciation when huge
33 volumes of meltwater and ice suddenly entered the Gulf of Mexico, the Arctic, and
34 Nordic Seas. For example, it was discovered several decades ago that an abrupt decrease
35 in the oxygen isotope ratio ($\delta^{18}\text{O}$) in surface-dwelling planktonic foraminifera midway
36 through deglaciation in the Gulf of Mexico was a signal of a fresh water flood⁴. The
37 source of this runoff must have been the decaying Laurentide Ice Sheet (LIS) via the
38 Mississippi River, but it ended abruptly at about 13 ka⁵. Kennett and Shackleton⁴
39 proposed that, as the southern margin of the LIS retreated northward, meltwater was
40 routed eastward to the Gulf of St. Lawrence, and the western North Atlantic. The $\delta^{18}\text{O}$
41 decrease in the Gulf of Mexico was more than 2 ‰, so a signal of 1 ‰ or more should
42 stand out in fresher, higher latitude waters. However, a low $\delta^{18}\text{O}$ signal at about 13 ka has
43 never been detected in high-quality sediment cores from the open western North
44 Atlantic^{6,7,8}, yet it is believed that the diversion of the flood from the Gulf of Mexico
45 interrupted deep ocean convection and caused the well-known Younger Dryas (YD) cold
46 episode (12.9-11.7 ka) in the North Atlantic region⁹. Other proposed explanations for the
47 origin of the YD include melting of the Fennoscandian ice sheet¹⁰, changes in
48 atmospheric circulation¹¹, and a combination of ice sheet melting, atmospheric flow
49 patterns, and radiative forcing¹². However, those explanations beg the question where
50 did the diverted meltwater go.

51 The YD was discovered near the beginning of the 20th Century as one of several
52 appearances of the Arctic wildflower *Dryas octopetala* in postglacial deposits in
53 Scandinavia^{13,14} and eventually was defined as a useful chronostratigraphic zone in the
54 North Atlantic region¹⁵. It was later proposed that meltwater routing and drainage pattern
55 changes could have caused the YD by lowering surface ocean salinity^{16,17}.

56 Recently, a glacial systems model showed that fresh water stored in glacial Lake
57 Agassiz most likely traveled north to the Beaufort Sea via Mackenzie River at 13 ka¹⁸,
58 and extensive field work on the Mackenzie Delta identified clear evidence of massive
59 flood deposits that occurred about the same time¹⁹. Although the exact timing and
60 magnitude of the Murton et al.¹⁹ conclusions have been questioned²⁰, application of a
61 high resolution ocean circulation model²¹ showed that, only when released to the Arctic
62 Ocean (via Mackenzie River), could the Lake Agassiz flood have caused the Younger
63 Dryas reduction of Atlantic meridional overturning circulation (AMOC)²² and
64 consequent northern hemisphere cooling.

65 Results and Discussion

66 Here we present data that show two events of substantial sea surface freshening
67 during deglaciation in newly acquired large diameter (jumbo) piston cores (JPCs) from
68 690 m on the continental slope ~100 km east of Mackenzie River (JPCs 15 and 27, Fig.
69 1). These and other new cores underlie the Atlantic water that enters the Arctic at Fram
70 Strait and the Barents Sea in the depth range ~100 to 800 m and circulates counter-
71 clockwise along the continental slopes²³. JPC-15 penetrated ~13 m of sediment and was
72 probably stopped by a coarse ice rafted debris (IRD) layer that has high magnetic
73 susceptibility, high Ca content (Fig. 2), and makes a prominent reflector in the acoustic

74 stratigraphy across the region (Fig. 3). Later, reoccupying the same site, a longer
75 (heavier) deployment (JPC-27) penetrated the deeper coarse layer. As these cores have
76 nearly identical lithology, we spliced them together to make a composite JPC-15/27 (Fig.
77 Extended Data (ED)1).

78 Compared to the lower layer, the upper coarse layer at this site is thicker, has
79 multiple events, and fewer IRD grains (Fig. 2), but each layer also has finer sand and silt
80 (Fig. 3). These data indicate that each coarse layer provides a record of enhanced
81 sediment transport to the upper slope of the Beaufort Sea. The two main events must be
82 the same that Scott et al.²⁴ noted in Canadian core PC-750 (Fig. 1). X-ray fluorescence
83 (XRF) counts of calcium (interpreted as detrital CaCO₃ content) show that our two events
84 have similar carbonate content, but also that lowest carbonate delivery to the region
85 occurred before the oldest event and was only a little higher between the events (Fig. 2).
86 Sediment deeper than ~5 m is faintly laminated at the cm scale, except for the massive
87 appearance of the first event (13.0-13.5 m). Laminae are better developed between 6 and
88 12 m, where about 300 were counted in XRF data (Fig. ED2).

89 As with the sediment and geophysical data, $\delta^{18}\text{O}$ on the polar planktonic
90 foraminifer *Neogloboquadrina pachyderma* (Ehrenberg) left coiling (Nps) in JPC-15/27
91 is marked by two prominent events at the same depths in the core (Fig. 2). At those
92 levels $\delta^{18}\text{O}$ of Nps ($\delta^{18}\text{O}_{\text{Nps}}$) decreased at least 1.0 ‰ below the ~2.0 ‰ baseline that
93 extends >4 m down the core. Above a pronounced maximum in $\delta^{18}\text{O}_{\text{Nps}}$ at 2-3 m, values
94 decrease by ~2.0 ‰ to the core top. We find the upper $\delta^{18}\text{O}_{\text{Nps}}$ minimum to the west of
95 JPC15/27 at JPC-09 (see ED), but not at other cores farther west (Figure 1). Benthic
96 foraminiferal (*Cassidulina neoteretis* Seidenkrantz) $\delta^{18}\text{O}$ at JPC15/27 yields a

97 stratigraphy more typical of the world ocean, with generally increasing values down the
98 core, although they are consistently low at about 5 m in the same samples where $\delta^{18}\text{O}_{\text{Nps}}$
99 is low (Fig. 2E).

100 Chronology

101 Chronology in Arctic sediments is uncertain because, although radiocarbon dating
102 of foraminifera is the simplest method, at present there is no way to know exactly the
103 near surface reservoir correction (ΔR) in the past. We made 14 accelerator mass
104 spectrometer (AMS) ^{14}C measurements on Nps from core 15 (Table ED1). Those dates
105 indicate maximum rates of sedimentation of at least 10 m per 1000 ^{14}C yrs between 6 and
106 12 m in the mid-deglacial interval of the core (Fig. 2F, ED3). Before and after that mid-
107 core extreme, rates are half that or less. We assume Nps calcified near the interface
108 between fresher, near-surface water and underlying saltier water, as it does today²⁵. In
109 that environment it was salty enough to survive but shallow enough to capture low $\delta^{18}\text{O}$
110 events. Six of the Nps dates were paired with dates on *C. neoteretis*. On average,
111 benthics are only 120 ± 220 yrs older than planktonics, including a result from 1300 m in
112 the Chukchi Sea (HLY0205 JPC-16, Fig. 1)²⁶. This small difference indicates upper
113 slope waters were relatively well ventilated.

114 For a calendar (calibrated) ^{14}C chronology, we need to choose a ΔR . In the
115 modern Arctic the Pacific inflow through Bering Strait is a source of old carbon that
116 would have been absent prior to about 11 ka when the strait was dry land^{26,27} (see Fig.
117 ED4 and further discussion). Bondevik et al.²⁸ showed that surface waters along the
118 Norwegian coast, which would have fed the Arctic, had a ΔR of about 0 yrs, like today,
119 during the Bølling-Allerød (B/A), about 100 yrs early in the YD, and about 200 yrs

120 during the mid-YD. Cao et al.²⁹ reached a similar conclusion based on U series dates and
121 ¹⁴C measurements on a solitary coral from the southern Labrador Sea, which would
122 monitor intermediate depth waters leaving the Nordic Seas. Therefore, we developed an
123 age model using a Bayesian method and $\Delta R = 0 \pm 100$ yrs for the Holocene and the
124 Allerød, and 200 ± 100 yrs for the YD (Fig. ED5). If the relatively high ΔR during the
125 YD was triggered by an event late in the Allerød, then the onset of that event should be
126 calibrated with a ΔR of ~ 0 years

127 These estimates of only a modest ΔR (0-200 years) encompass the pre-bomb
128 estimate³⁰ based on ¹⁴C, tritium, and $\delta^{18}\text{O}$ on samples collected decades ago when bomb
129 produced nuclides were beginning to invade the deep Arctic. Ostlund et al.³⁰ inferred the
130 pre-bomb ¹⁴C activity of waters between 500 and 1500 m was about -55 ± 5 ‰, giving a
131 ΔR of ~ 40 yrs (Fig. 4). Therefore, although deep-water ¹⁴C circulation in the Arctic may
132 have been very different in the past^{31,32}, it appears that the ¹⁴C ventilation of upper waters
133 (<1500 m) in the Canada Basin was similar to today.

134 Our age model gives interpolated calendar ages in JPC-15/27 of 12.94 ± 0.15 ka
135 for the onset of the upper $\delta^{18}\text{O}$ minimum (constrained by dates of 13.06 ka at 520 cm and
136 12.66 ka at 500 cm; Table ED1), and ~ 14.6 ka for the peak of the older one (Fig. 5). The
137 age of the older event and its associated IRD is consistent with the ages (15.2-14.1 ka)
138 reported for the initial withdrawal of ice streams from Amundsen Gulf and M'Clure
139 Strait³³. The age for the onset of the later freshening in the Beaufort Sea (12.94 ± 0.15
140 ka) is virtually the same as the beginning of the Younger Dryas at 12.85 ± 0.14 ka in
141 Greenland ice cores³⁴, and identical to the end of freshening in the Gulf of Mexico (12.94
142 ± 0.17 ka) (Fig. 5). Minimum $\delta^{18}\text{O}$ in JPC-15/27 first occurred at 12.59 ± 0.14 ka, within

143 uncertainty of the equivalent event at JPC-09 (12.7 ± 0.10 ka). The coincidence of the
144 end of flooding in the Gulf of Mexico and the onset of flooding in the eastern Beaufort
145 Sea is strongly suggestive that the routing of meltwaters³⁵ switched from the Gulf of
146 Mexico to the Beaufort Sea at about 13 ka.

147 Ocean and climate change in Beaufort Sea

148 Our composite sequence from the continental slope east of Mackenzie River
149 began around 15-16 ka with modest ice rafting from local sources such as ice streams in
150 M'Clure Strait and Amundsen Gulf. Icebergs would have traveled clockwise around
151 Canada Basin via the Beaufort Gyre, and the counter clockwise shelfbreak current³⁶
152 would have been weakened with sea level below the depth of Bering Strait. Mackenzie
153 River may not have supplied substantial detrital carbonate because the extensive
154 Devonian carbonate terrain south of Great Slave Lake and north of Ft. McMurray³⁷ was
155 probably ice-covered, but it may have been a source of runoff and sediment at least since
156 ~18 ka based on the background low $\delta^{18}\text{O}$ (Fig. 5). This was a time when secular change
157 in the ocean due to increased ice volume was about +1 ‰, indicating the sea surface was
158 less saline than today by at least 1 psu, assuming the modern $\delta^{18}\text{O}$ -salinity relationship³⁸.
159 This setting prevailed until ~14.6 ka, when ice rafting dramatically increased from
160 Amundsen Gulf and M'Clure Strait, and $\delta^{18}\text{O}_{\text{Nps}}$ decreased by >1 ‰. The five samples
161 defining this minimum were probably deposited within decades.

162 At the end of the 14.6 ka event, Amundsen Gulf probably remained a source of
163 sediment to the continental slope in the eastern Beaufort Sea until the ice stream was
164 fully retreated. Mackenzie River may have always been a large source of sediment, but
165 as more of its watershed north of Fort McMurray was deglaciated, the more important it

166 must have become. The laminated sediments, high sedimentation rate, and general lack of
167 coarse particle ice rafting suggest large sediment input from the Mackenzie River
168 between 13.5 and ~14.4 ka (6-12 m in the core). The high sedimentation rates along the
169 slope may be explained by discharge over bottom fast ice on the shelf, which could
170 efficiently transport sediment farther seaward (e.g., ref 39). Based on the diagnostic
171 acoustic signature of the rapidly emplaced Bølling-Allerød section (Fig. 3), the western
172 extent of the deposit pinches out between JPC-09 and JPC-06 (Fig. 1, Fig. ED8). Counts
173 of ~300 layers within the ~900 year interval where sedimentation rates are highest show
174 the layers are probably not annual (Fig. ED2). The interval between the two $\delta^{18}\text{O}_{\text{Nps}}$
175 minima represents most of the Bølling-Allerød climate warming, when the AMOC was
176 almost as strong as today²², but evidently the lowered salinity in the Beaufort Gyre had
177 little direct influence on North Atlantic overturning. This may indicate that the gyre was
178 in a mostly anticyclonic state, which today stores ice and fresh water⁴⁰.

179 Close to 13 ka the rapid increase in magnetic susceptibility and decreased $\delta^{18}\text{O}_{\text{Nps}}$
180 in JPC-15/27 herald the beginning of the YD. Although the two $\delta^{18}\text{O}_{\text{Nps}}$ minima in this
181 core are similar in size, the YD event was more likely to have been a flood of fresh water
182 with high suspended load¹⁹ because $\delta^{18}\text{O}$ of *C. neoteretis*, living at the seafloor, decreased
183 in exactly the same samples as Nps during the ~13 ka but not the earlier event. This, we
184 propose, may record a hyperpycnal flow that brought low salinity to the seafloor and that
185 would be more likely from a river flood. The major sediment depocenter in this model
186 must be farther seaward because sedimentation rates drop during this time interval at 690
187 m water depth (Fig. 2). The YD flood can be traced to the west as far as core JPC-09
188 using $\delta^{18}\text{O}_{\text{Nps}}$, but the signal is not clear west of that at JPC-06, and neither the $\delta^{18}\text{O}$

189 minima nor the maximum in magnetic susceptibility are evident as far west as JPC-02
190 near Barrow, Alaska (Fig. ED7).

191 About 200 yrs after the onset of the YD flood all four sediment and isotope
192 proxies were briefly aligned in the first (labeled “a”) of several sub-events (Fig. 2 A-D).
193 The low $\delta^{18}\text{O}_{\text{Nps}}$ episode is mostly centered between the subpeaks “a” and “b” of the
194 magnetic susceptibility (12.8 to 12.3 ka), but the last of the spikes in IRD and carbonate
195 deposition ended with increased $\delta^{18}\text{O}_{\text{Nps}}$ at the end of flooding. Maximum $\delta^{18}\text{O}_{\text{Nps}}$ at
196 ~ 12.2 ka probably marks an interval of relatively high salinity in the near surface
197 Beaufort Sea⁴¹, followed by more typical decreasing $\delta^{18}\text{O}$ trends in benthic and
198 planktonic foraminifera as ice volume decreased and climate warmed during the
199 Holocene. The lingering high magnetic susceptibility late in the YD may indicate
200 evolving sources of sediment from Mackenzie River, and it might also relate to evidence
201 of a second flood ~ 11 ka (ref. 19).

202 Knowing the duration of the YD flood is important for calculating the fresh water
203 transport and evaluating its effect on the AMOC. If we take the main flood interval of
204 the YD as that part where $\delta^{18}\text{O}_{\text{Nps}}$ was less than the 2 ‰ baseline, then it lasted ~ 660
205 years. If the lowest $\delta^{18}\text{O}_{\text{Nps}}$ indicates peak discharge, then most of the fresh water
206 transport could have occurred in about 130 years (Table ED3). However, it must be kept
207 in mind that if the Mackenzie River choke point at Fort McMurray was breached
208 suddenly at the beginning of the YD, and this is contentious⁴², then the outburst of
209 Glacial Lake Agassiz water would have probably produced initial salinities over our core
210 site that were too low for Nps to grow. Furthermore, estimates of very high fresh water
211 transport during the flood are based on the assumption that it occurred on the timescale of

212 a year⁴³, yet if the main flood was that brief then it is unlikely enough planktonic
213 foraminifera could have recorded the low $\delta^{18}\text{O}$ to leave a signal in the geological record.

214 Most likely the initial Mackenzie discharge at 12.9 ka was a combination of both
215 a routing change from the Gulf of Mexico and an outburst flood from glacial Lake
216 Agassiz. This potent combination of two sources of fresh water was probably effective in
217 reducing the AMOC³⁵, especially considering it was an Arctic source²¹. However, even
218 if the combined routing plus glacial lake release to Mackenzie River itself was too
219 modest to trigger a collapse of the AMOC, many large rivers empty into the Arctic², and
220 Lena River, one of the largest, also flooded about 13 ka (ref 44). Finally, it should be
221 noted that in addition to fresh water floods in the Arctic around the beginning of the YD,
222 it is reported that enhanced sea ice export through Fram Strait at that time also had a
223 Beaufort Sea source⁴⁵.

224 By the onset of the YD, the AMOC may have already been close to a tipping
225 point after ~1500 years of low salinity leakage from the Beaufort Sea, and transport to the
226 nearshore convective regions of the Nordic seas^{46,47}. Increased freshening has also been
227 noted at other coastal locations in the North Atlantic, including the proposed eastern
228 outlet (St. Lawrence River system) using various proxies^{48,49,50}, the Baltic Sea^{10, 51}, and
229 off eastern Greenland where $\delta^{18}\text{O}_{\text{Nps}}$ minima of YD age are thought to reflect local
230 melting⁵² but could also be evidence of the Mackenzie flood. The coincidence of
231 decreased $\delta^{18}\text{O}$ in the Beaufort Sea and increased $\delta^{18}\text{O}$ in the Gulf of Mexico near the
232 beginning of the YD is a good test of the meltwater diversion hypothesis of Kennett and
233 Shackleton⁴ (Fig. 5). Considering all the other observations, including the climatic
234 background suggested by alternative hypotheses¹⁰⁻¹² that may have helped sustained the

235 event, and the lack of a large YD minimum in $\delta^{18}\text{O}$ anywhere in the open North Atlantic
236 Ocean, the ~12.9 ka flood of Mackenzie River was most likely the trigger for the
237 reduction of the AMOC and Younger Dryas cooling.

238 References

- 239 1. Dickson, R. R., Meincke, J., Malmberg, S. A. & Lee, A. J. The "Great Salinity
240 Anomaly" in the Northern North Atlantic 1968-1982. *Prog. Oceanog.* **20**, 103-
241 151 (1988).
- 242 2. Aagard, K. & Carmack, E. The role of sea ice and other fresh water in the Arctic
243 circulation. *Jour. Geophys. Res.* **94**, 14485-14498 (1989).
- 244 3. Häkkinen, S. An Arctic source for the great salinity anomaly: A simulation of the
245 Arctic ice-ocean system for 1955-1975. *Jour. of Geophys. Res.* **98**, 16,397-
246 316,410 (1993).
- 247 4. Kennett, J. P. & Shackleton, N. J. Laurentide ice sheet meltwater recorded in Gulf of
248 Mexico deep-sea cores. *Science* **188**, 147-150 (1975).
- 249 5. Williams, C., Flower, B. & Hastings, D. W. Seasonal Laurentide ice sheet melting
250 during the "Mystery Interval" (17.5-14.5 ka). *Geology* **40**, 955-958 (2012).
- 251 6. Keigwin, L. D. & Jones G. A. The marine record of deglaciation from the continental
252 margin off Nova Scotia. *Paleoceanography* **10**, 973-985 (1995).
- 253 7. de Vernal, A., Hillaire-Marcel, C. & Bilodeau, G. Reduced meltwater outflow from
254 the Laurentide ice margin during the Younger Dryas. *Nature* **381**, 774-777
255 (1996).

- 256 8. Keigwin, L. D., Sachs, J., Rosenthal, Y. & Boyle, E. A. The 8200 year B.P. event in the
257 slope water system, western subpolar North Atlantic. *Paleoceanography* **20**,
258 doi:10.1029/2004PA001074 (2005).
- 259 9. Broecker, W. S., et al. The routing of meltwater from the Laurentide ice-sheet
260 during the Younger Dryas cold episode. *Nature* **341**, 318-321 (1989).
- 261 10. Muschitiello, F. et al. Fennoscandian freshwater control on Greenland
262 hydroclimate shifts at the onset of the Younger Dryas. *Nature Comm.* (2015).
- 263 11. Brauer, A. Haug, G.H., Dulski, P., Sigman, D. M., & Negendank, J. F. W. An abrupt
264 wind shift in western Europe at the onset of the Younger Dryas cold period.
265 *Nature Geoscience* **1**:520-523 (2008).
- 266 12. Renssen, H. et al. Multiple causes of the Younger Dryas cold period. *Nature*
267 *Geoscience* **8**, 946-950 (2015).
- 268 13. Andersson, G. Swedish vegetation history. Stockholm, P.A. Norstedt & Soners
269 Forlag (1897).
- 270 14. Hartz, N. & Milthers, V. The late glacial clay in the Allerød brickyard. *Meddelelser*
271 *Dansk Geologisk Foreningen* **8**, 31-60 (1901).
- 272 15. Mangerud, J., Andersen, S. T., Berglund, B. E., & Donner, J. J. Quaternary
273 stratigraphy of Norden, a proposal for terminology and classification. *Boreas*
274 **3**, 110-127 (1974).
- 275 16. Johnson, R. G. & McClure B. T. A model for northern hemisphere continental ice
276 sheet variation. *Quaternary Res.* **6**, 325-353 (1976).
- 277 17. Rooth, C. Hydrology and ocean circulation. *Prog. Oceanog.* **11**, 131-149 (1982).

- 278 18. Tarasov, L. & Peltier, W. R. Arctic freshwater forcing of the Younger Dryas cold
279 reversal. *Nature* **435**, 662-665 (2005).
- 280 19. Murton, J. B., Bateman, M. D., Dallimore, S. R., Teller, J. T. & Yang, Z. Identification
281 of Younger Dryas outburst flood path from lake Agassiz to the Arctic Ocean.
282 *Nature* **464**, 740-743 (2010).
- 283 20. Carlson, A.E. et al. Geochemical proxies of North American freshwater routing
284 during the Younger Dryas cold event. *Proc. Nat. Acad. Sci.* **104**, 6556-6561
285 (2007).
- 286 21. Condron, A. & Winsor, P. Meltwater routing and the Younger Dryas. *Proc. Nat.*
287 *Acad. Sci.* doi:10.1073/pnas.1207381109 (2012).
- 288 22. McManus, J. F., Francois, R., Gherardi, J.-M., Keigwin, L. D. & Brown-Leger, S.
289 Collapse and rapid resumption of Atlantic meridional circulation linked to
290 deglacial climate changes. *Nature* **428**, 834-837 (2004).
- 291 23. Rudels, B., Jones, E. P., Anderson, L. G. & Kaattner, G. On the intermediate depth
292 waters of the Arctic Ocean. *Geophysical Monograph* **85**, 33-46 (1994).
- 293 24. Scott, D., Schell, T., St-Onge, G., Rochon, A. & Blasco, S. Foraminiferal assemblage
294 changes over the last 15,000 years on the Mackenzie-Beaufort Sea slope and
295 Amundsen Gulf, Canada: Implications for past sea ice conditions.
296 *Paleoceanography* **24** (doi:10.1029/2007PA001575) (2009).
- 297 25. Bauch, D., Carstens, J. & Wefer, G. Oxygen isotope composition of living
298 *Neogloboquadrina pachyderma* (sin.) in the Arctic Ocean. *Earth Planet. Sci.*
299 *Lett.* **146**, 47-58 (1997).

- 300 26. Keigwin, L. D, Donnelly, J. P., Cook, M.S., Driscoll, N.W. & Brigham-Grette, J.
301 Flooding of Bering Strait and Holocene climate in the Chukchi Sea. *Geology*
302 **34**, 861-864 (2006).
- 303 27. Jakobsson, M. et al. Post-glacial flooding of the Beringia Land Bridge dated to
304 11,000 cal yrs BP based on new geophysical and sediment records. *Clim. Past*
305 *Discuss.*, doi:10.5194/cp-2017-11 (2017).
- 306 28. Bondevik, S., Mangerud, J., Birks, H. H., Gulliksen, S. & Reimer, P. Changes in
307 North Atlantic radiocarbon reservoir ages during the Allerod and Younger
308 Dryas. *Science* **312**, 1514-1517 (2006)
- 309 29. Cao, L., Fairbanks, R.G., Mortlock, R.A. & Risk M.A. Radiocarbon reservoir age of
310 high latitude North Atlantic surface water during the last deglacial. *Quat. Sci.*
311 *Rev.* **26**, 732-742 (2007).
- 312 30. Ostlund, H., Possnert, G. & Swift, J. Ventilation rate of the deep Arctic Ocean from
313 carbon 14 data. *Jour. Geophys. Res.* **92**, 3769-3777 (1987).
- 314 31. Cronin, T. et al. Deep Arctic Ocean warming during the last glacial cycle. *Nature*
315 *Geoscience* **5**, 631-634 (2012).
- 316 32. Thornalley, D. J. R. et al. A warm and poorly ventilated deep Arctic
317 Mediterranean during the last glacial period. *Science* **349**, 706-710 (2015).
- 318 33. Stokes, C. R., Clark, C. D. & Storrar, R. Major changes in ice stream dynamics
319 during deglaciation of the north-western margin of the Laurentide ice sheet.
320 *Quat. Sci. Rev.* **28**, 721-738 (2009).
- 321 34. Rasmussen, S., et al. A new Greenland ice core chronology for the last glacial
322 termination. *Jour. Geophys. Res.* **111**, doi:10.1029/2005JD006079 (2006).

- 323 35. Meissner, K. & Clark, P. Impact of floods versus routing events on the
324 thermohaline circulation. *Geophys. Res. Lett.* **33**, doi:10.1029/2006GL026705
325 (2006).
- 326 36. von Appen, W.-J. & Pickart, R. Two configurations of the western Arctic
327 Shelfbreak Current in summer. *Jour. Phys. Oceanography* **42**, 329-351 (2012).
- 328 37. Wheeler, J., et al. Geological Map of Canada. "A" Series Map 1860A;
329 doi:10.4095/208175, Geological Survey of Canada (1996).
- 330 38. Cooper, L., et al. Linkages among runoff, dissolved organic carbon, and the stable
331 oxygen isotope composition of seawater and other water mass indicators in
332 the Arctic Ocean. *Jour. Geophys. Res.* **110**, (doi:10.1029/2005JG000031)
333 (2005).
- 334 39. Macdonald, R. & Yu, Y. The Mackenzie estuary of the Arctic Ocean. *Handbook of*
335 *Environmental Chemistry*. Berlin, Springer-Verlag. **5**: 91-120 (2006).
- 336 40. Proshutinsky, A. & Johnson, M.A. Two circulation regimes of the wind-driven
337 Arctic Ocean. *Jour. Geophys. Res.* **102**, 12493-12514 (1997).
- 338 41. Schell, T., Scott, D. B., Rochon, A. & Blasco, S. Late Quaternary paleoceanography
339 and paleo-sea ice conditions in the Mackenzie Trough and Canyon, Beaufort
340 Sea. *Can. J. Earth Sci.* **45**, 1399-1415 (2008).
- 341 42. Fisher, T.G., Waterson, N., Lowell, T. V. & Hajdas, I. Deglaciation ages and
342 meltwater routing in the Fort McMurray region, northeastern Alberta and
343 northwestern Saskatchewan, Canada. *Quat. Sci. Rev.* **28**, 1608-1624 (2009).

- 344 43. Leverington, D. W., Mann, J. D. & Teller, J. T. Changes in the bathymetry and
345 volume of glacial Lake Agassiz between 11,000 and 9300 ¹⁴C yr B.P.
346 *Quaternary. Res.* **54**, 174-181 (2000).
- 347 44. Spielhagen, R.F., Erlenkeuser, H. & Siegert, C. History of freshwater runoff across
348 the Laptev Sea (Arctic) during the last deglaciation. *Global and Planetary*
349 *Change* **48**, 187-207 (2005).
- 350 45. Hillaire-Marcel, C., Maccali, J., Not, C. & Poirier, A. Geochemical and isotopic
351 tracers of Arctic sea ice sources and export with special attention to the
352 Younger Dryas interval. *Quat. Sci. Rev.* **79**, 184-190 (2013).
- 353 46. Mauritzen, C. Production of dense overflow waters feeding the North Atlantic
354 across the Greenland-Scotland Ridge. Part 1: Evidence for a revised
355 circulation scheme. *Deep-Sea Res.* **43**, 769-806 (1996).
- 356 47. Pedlosky, J. & Spall, M. Boundary intensification of vertical velocity in a beta-
357 plane basin. *Jour. Phys. Oceanography* **35**, 2487-2500 (2005).
- 358 48. Carlson, A.E. & Clark, P.U. Ice sheet sources of sea level rise and freshwater
359 discharge during the last deglaciation. *Rev. Geophys.* **50** (2011RG000371)
360 (2012).
- 361 49. Cronin, T.M., Rayburn, J.A., Guilbault, J.-P. & Thunell, R. Stable isotope evidence
362 for glacial lake drainage through the St. Lawrence estuary, eastern Canada,
363 ~13.1-12.9 Ka. *Quat. International* **260**, 55-65 (2012).
- 364 50. Levac, E., Lewis, M., Stretch, V., Duchesne, K. & Neulieb, T. Evidence for
365 meltwater drainage via the St. Lawrence River valley in marine cores from

- 366 the Laurentian Channel at the time of the Younger Dryas. *Global and*
367 *Planetary Change* **130**, 47-65 (2015).
- 368 51. Boden, P., Fairbanks, R.G., Wright, J. D. & Burckle, L. H. High-resolution stable
369 isotope records from southwest Sweden: The drainage of the Baltic Ice Lake
370 and Younger Dryas ice margin oscillations. *Paleoceanography* **12**, 39-49
371 (1997).
- 372 52. Jennings, A.E, Hald, M., Smith, M. & Andrews, J.T. Freshwater forcing from the
373 Greenland Ice Sheet during the Younger Dryas: evidence from southeastern
374 Greenland shelf cores. *Quat. Sci. Rev.* **25**, 282-298 (2006).
- 375 53. Jakobsson, M. et al. The International bathymetric chart of the Arctic Ocean
376 (IBCAO) version 3.0. *Geophys. Res. Lett.* Doi: 10.1029/2012GL052219
377 (2012).
- 378 54. Leventer, A., Williams, D. F. & Kennett, J. P. Dynamics of the Laurentide ice sheet
379 during the last deglaciation: evidence from the Gulf of Mexico. *Earth and*
380 *Planet. Sci. Lett.* **59**,11-17 (1982).

381

382 **Acknowledgements** We thank the officers and crew of USCGC Healy for making this
383 project a success. We are also indebted to M. Carman for help processing core samples;
384 A. McNichol for helpful discussions of ^{14}C in the Arctic; A. Gagnon for the stable
385 isotope measurements; the NOSAMS staff for providing ^{14}C data; M. McCarthy, C.
386 Moser, C. Griner, and C. Mayo for leading the coring effort. S. Nielsen helped with
387 translation of ref. 14. The manuscript benefited from comments of 4 anonymous
388 reviewers [and help from M. Blaauw and B. Keigwin with the Bayesian age model](#). This

389 research was funded by NSF grants ARC 1204045 to L.D.K., and ARC 1203944 to
390 N.W.D.

391

392 **Author Contributions** L.D.K. conceived the project, N.W.D. and S.K surveyed the
393 seafloor, identified coring locations, and studied grain size; B.R. conducted the magnetic
394 measurements; and N.Z. and L.G. conducted the XRF scanning. All authors helped write
395 the manuscript.

396 **Author Information** Reprints and permissions information is available at [www.](http://www.nature.com/reprints)
397 [nature.com/reprints](http://www.nature.com/reprints). The authors have no competing financial interests. Correspondence
398 and requests for materials should be addressed to lkeigwin@whoi.edu

399 **Methods**

400 Site survey methods, laminae counting methods, core sampling and stable isotope
401 methods, sample preparation for radiocarbon dating, and Bayesian age modeling
402 are presented in Supplementary Information sections 1, 2, 3, 4.2, and 4.4.

403 **Data Availability:**

404 Radiocarbon data appear in Extended Data Table 1, and stable isotope data appear
405 in Extended Data Table 3. The Fe/Ca and magnetic data are available from the
406 authors upon request.

407 **Code availability:**

408

409 The code for the bacon age model is freely available;

410 see <http://chrono.qub.ac.uk/blaauw/bacon.html>. The settings used are found in

411 Supplementary Section 4.4.

412

413

Figure Captions

414 **Fig. 1.** Overview of core locations and stratigraphy in the eastern Beaufort Sea. (Top)
415 Track of USCGC Healy cruise 1302 with location of JPC sites (yellow) and other cores
416 (red) discussed in this study. Inset (based on ref 27) shows the study area with respect to
417 the Arctic Ocean. LR=Lomonosov Ridge, CB=Chukchi Borderland, BC=Barrow
418 Canyon, MT=Mackenzie Trough, AG=Amundsen Gulf, MS=M'Clure Strait, BI=Banks
419 Island, VI=Victoria Island. Based on low $\delta^{18}\text{O}_{\text{Nps}}$ and seismic evidence, the YD flood
420 deposit (sites in yellow with a cross) ranges from JPC-09 in the west to JPC-22 in the
421 east. Because of Coriolis force and lowered sea level, the flood would have travelled
422 north and east. (Bottom) Down core magnetic susceptibility is shown delineating the
423 Holocene (yellow) - Deglacial (blue) boundary. Selected AMS ^{14}C dates are calibrated
424 ka.

425

426 **Fig. 2.** Proxy data from JPC-15/27 in the eastern Beaufort Sea. Magnetic susceptibility
427 (A), lithic particle abundance (B), Ca content (proxy for CaCO_3) (C), and $\delta^{18}\text{O}_{\text{Nps}}$ (D) all
428 exhibit extreme values early the Bolling/Allerod warming at 14.6 ka (red line at 1300 cm)
429 and during the YD (11.7-12.9 ka) (~380-510 cm). Dashed vertical lines correlate smaller
430 features. Dashed horizontal line in (D) is a ~2.0 ‰ reference for $\delta^{18}\text{O}$ features. Data
431 corresponding to a large dropstone at 1346-1355 cm excluded from C. The *C. neoteretis*
432 (benthic) $\delta^{18}\text{O}$ (E) is unremarkable except that the clear minimum ~450-500 cm occurs in
433 the same samples as the low $\delta^{18}\text{O}_{\text{Nps}}$. Sedimentation rates (F) are very high where
434 sediments are laminated, although ^{14}C dates exaggerate the B/A maximima (Figure
435 ED2),.

436

437 **Fig. 3.** Grain size variability down composite jumbo piston core JPC15/27. Magnetic
438 susceptibility data are superposed on the grain size and the seismic data, assuming the
439 pressure wave velocity of the core logged at sea (1333 ms^{-1}). These properties all vary
440 together. The seismic data show a diagnostic reflector pattern with an upper ($\sim 380\text{-}520$
441 cm) and lower high (~ 1320 cm) amplitude reflectors that bound a region of lower
442 acoustic reflectivity. The zone of lower reflectivity correlates with high sediment
443 accumulation rates, low magnetic susceptibility, low ice rafted debris (IRD), and low Ca
444 content (Fig. 2).

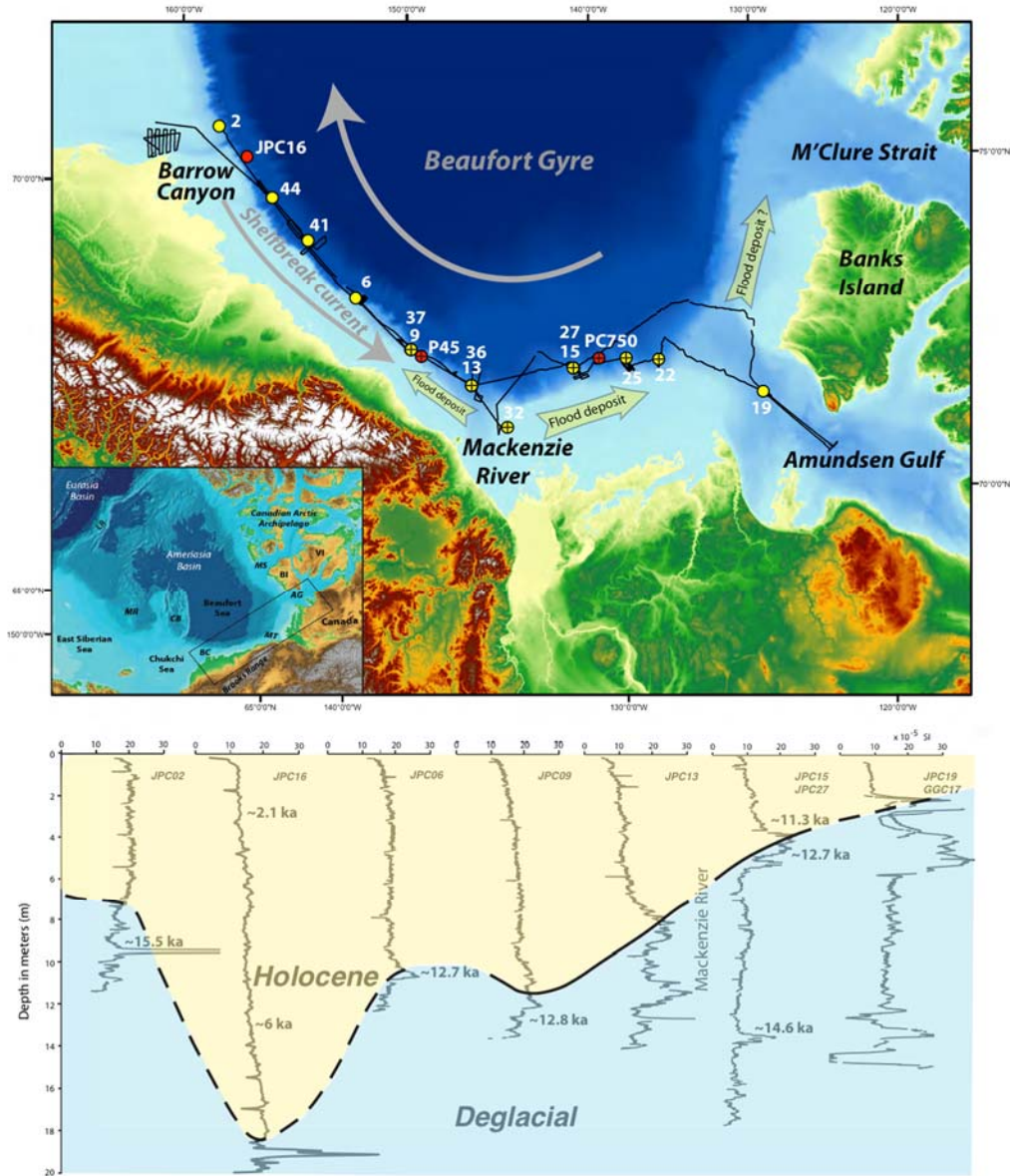
445

446 **Fig. 4.** Radiocarbon basis for the age model in this paper. Ostlund et al.³⁰ synthesized
447 $\Delta^{14}\text{C}$, $\delta^{18}\text{O}$, and tritium data collected from several Arctic ice camps (LOREX, CESAR,
448 AIWEX) between 1977 and 1985 and concluded that the pre-bomb value of intermediate
449 depth waters (500 to 1500 m) was $-55 \pm 5 \text{ ‰}$ (vertical black line $\pm 1\sigma$ (dashed)), and pre-
450 bomb shelf water was $-48 \pm 3 \text{ ‰}$ (triangle). The ice camp results are considered to be
451 equivalent to Canada Basin water in that all are on the west side of Lomonosov Ridge.
452 Our age model uses $\Delta R = 0 \pm 100$ (1σ) for the Holocene and Bolling/Allerod, within
453 uncertainty of the pre-bomb estimate³⁰, but we use a larger ΔR for the YD (200 ± 100)
454 (Fig. ED5).

455

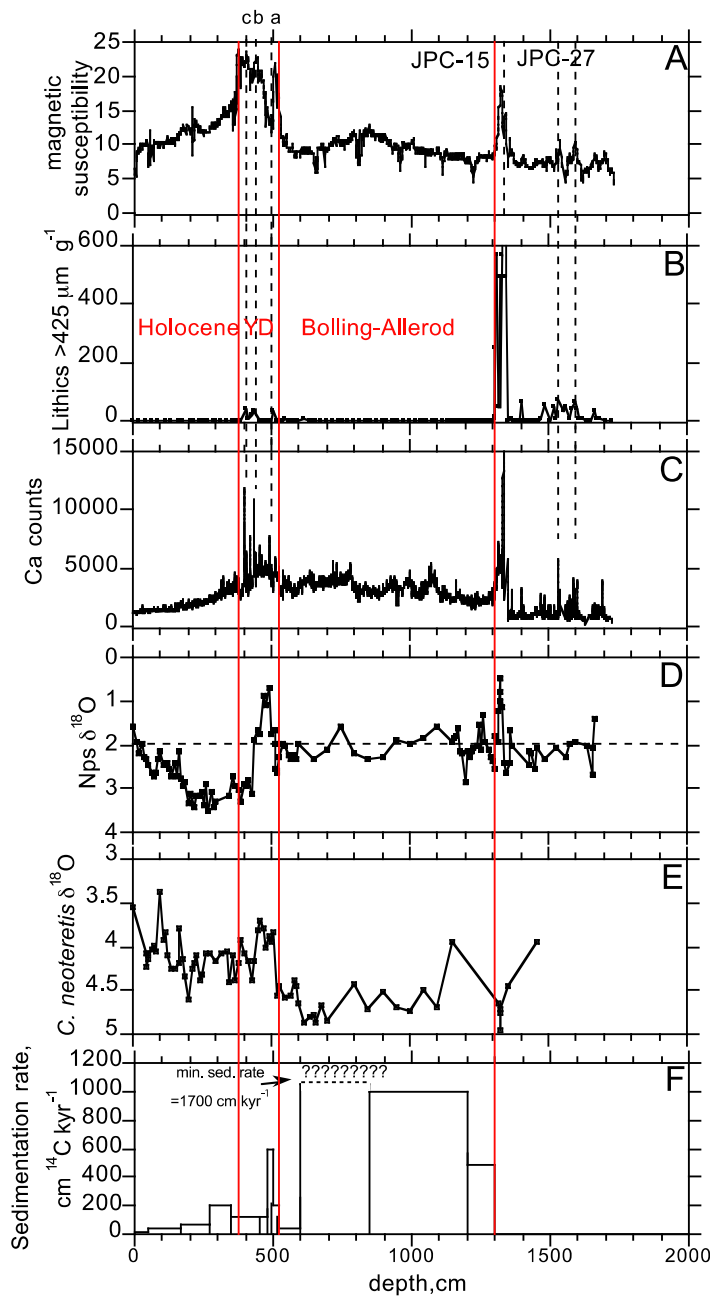
456 **Fig. 5.** Comparison of deglacial $\delta^{18}\text{O}$ between Orca Basin in the Gulf of Mexico and
457 Beaufort Sea. Arctic data are based on *N. pachyderma* (s) (blue squares, core 15/27; red
458 line, JPC-09) and Orca Basin data are based on the planktonic foraminifer

459 *Globigerinoides ruber* (green line, Williams et al.⁵; black squares, Leventer et al.⁵⁴) (see
460 ED for chronology details of the Leventer et al. core). The eastern Beaufort Sea
461 freshened at about 12.9 ka coincident with the end of Gulf of Mexico freshening and
462 consistent with the hypothesis that meltwater was diverted from the Gulf to a more
463 northern outlet as deglaciation progressed⁴. YD= Younger Dryas, B/A = Bolling/Allerod,
464 HS-1 = Heinrich Stadial 1, LGM = last glacial maximum.
465



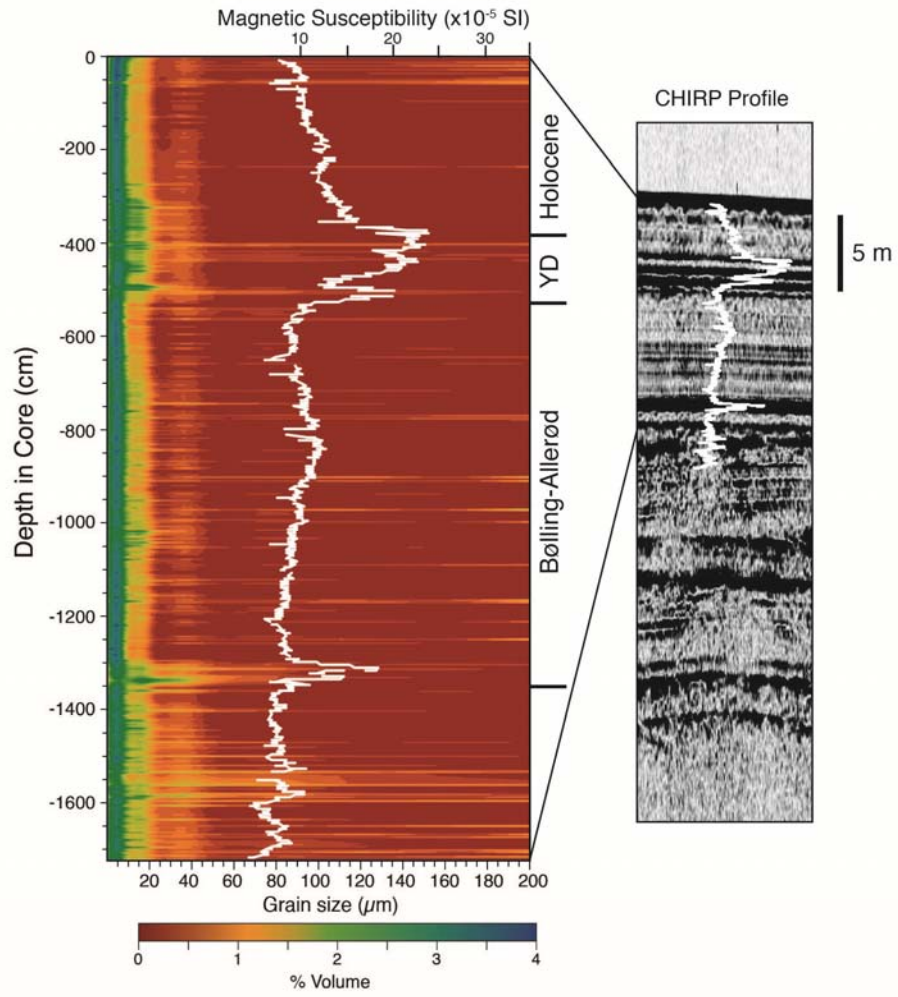
466
 467
 468
 469
 470

Figure 1

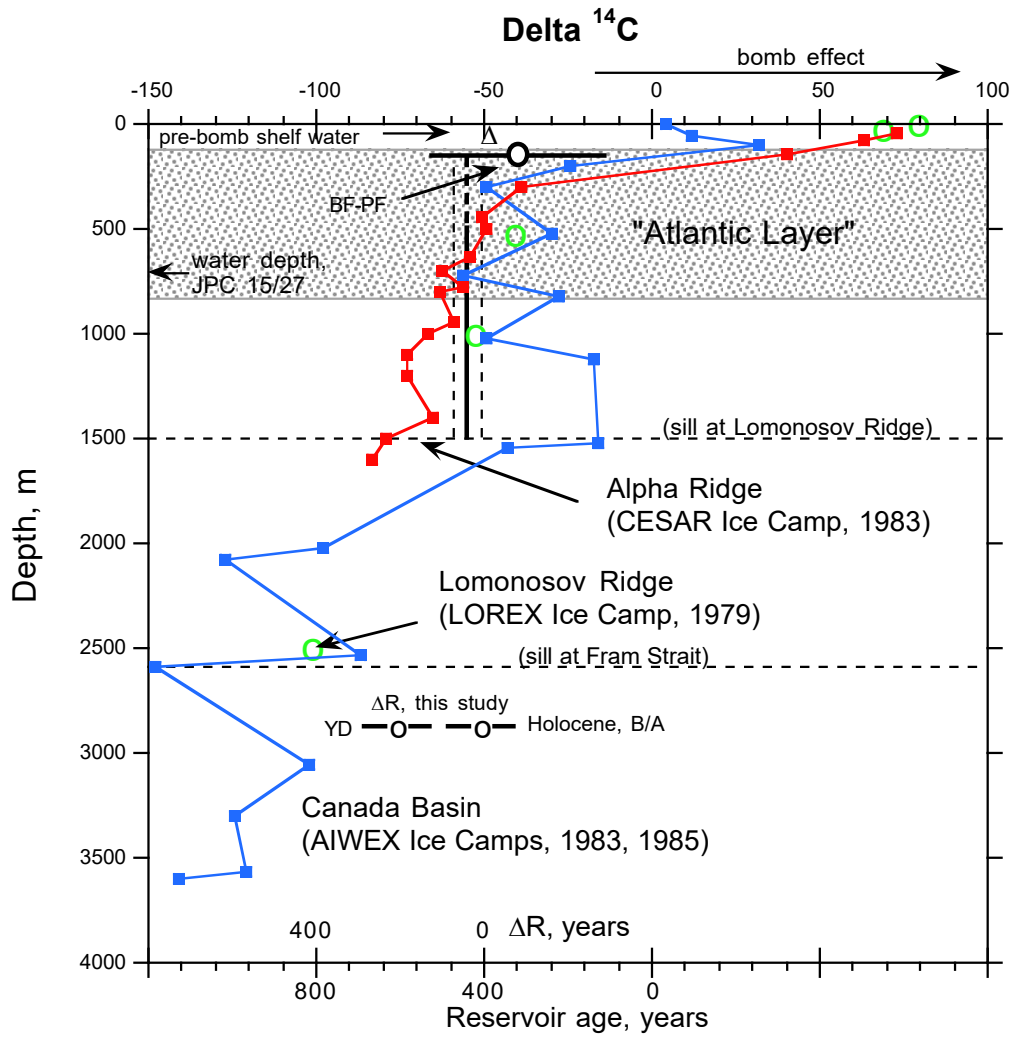


471
 472
 473
 474

Figure 2

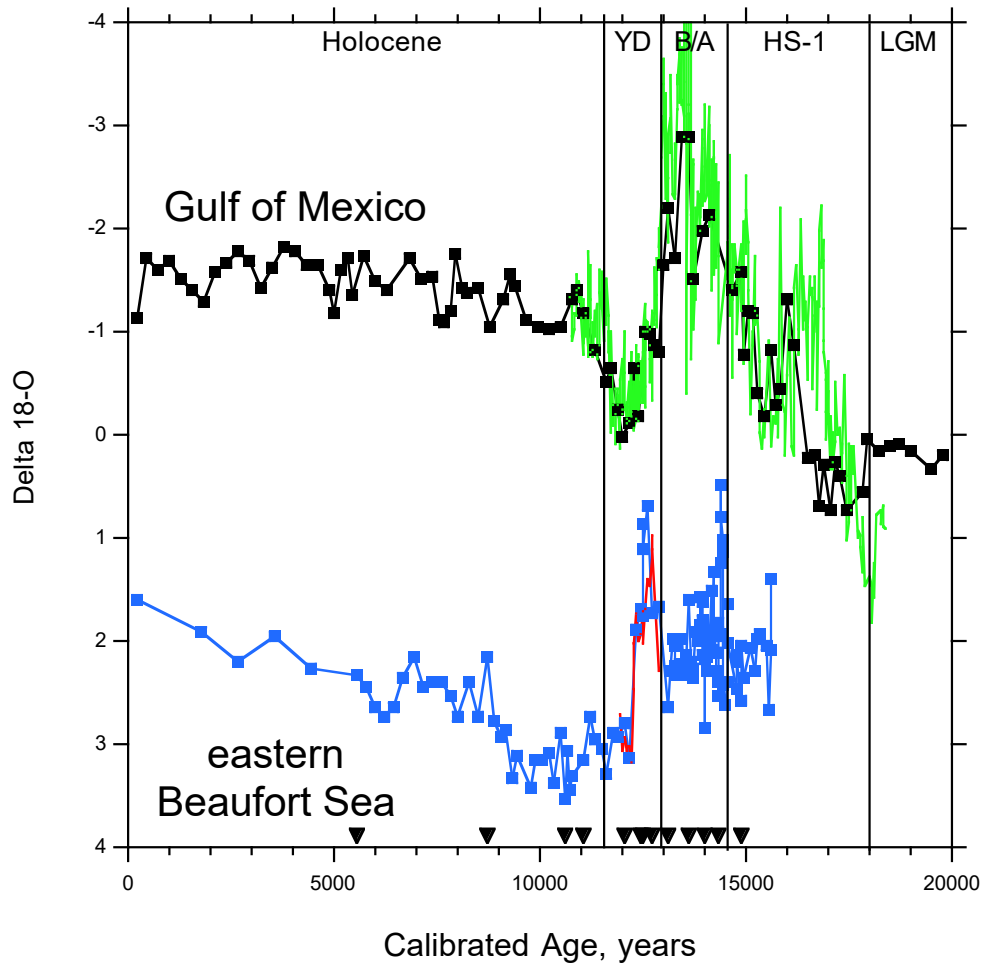


475
 476 Figure 3
 477



478
 479
 480
 481

Figure 4



482
483
484
485

Figure 5

486

Deglacial Floods in the Beaufort Sea Preceded Younger Dryas Cooling

488

Supplementary Information

489

490

Extended Data

491

1. Site surveying

493

494

Sites were surveyed on USCGC Healy using the hull mounted multibeam swath bathymetry system, and a Knudsen 320B/R sonar. The Knudsen system, also hull mounted, operates at a central frequency of 3.5 kHz and sweeps between 2 and 6 kHz which makes it “chirp.”

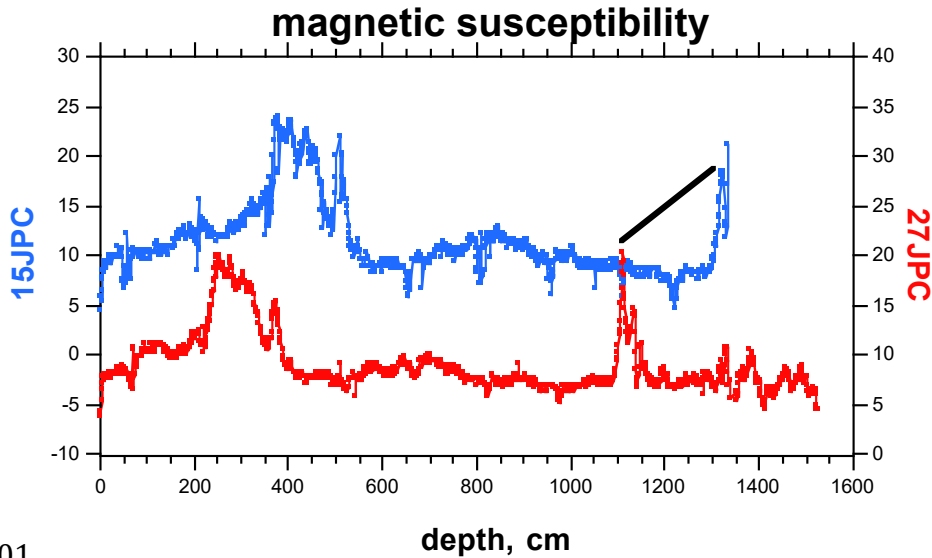
497

498

2. Stratigraphy

499

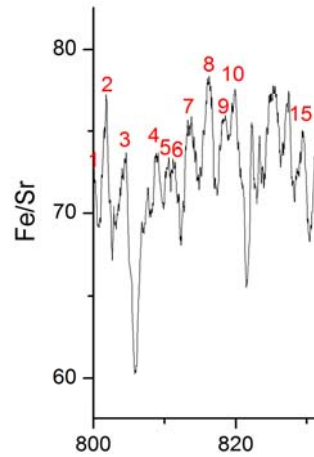
500



501

Fig. ED1. Magnetic susceptibility records of HLY1302 cores JPC15/27 from the same location at 690 m on the continental slope east of Mackenzie River (JPC15: 71°06.222'N, 135°08.129'W; JPC27: 71°06.360'N, 135°09.640'W). To make a 1729 cm composite section, we patched to JPC-15 at 1329 cm the data below 1125 cm in JPC-27 (with a +205 cm offset).

502
503
504
505
506
507
508



509

510

511 3. Sampling and 512 stable isotopes

513 Core JPC15
514 was initially chosen
515 for study because of
516 its position east of
517 Mackenzie Trough
518 and because of its

Fig. ED2. Laminae counted using Fe/Sr variability of a one-meter section in HLY1302 JPC15. Many other elemental pairs show similar variability. High Fe/Sr suggests greater terrestrial content. The resolution of the data is 0.4 mm and the data are smoothed with a 19-point running mean. There are about 50 peaks in this section with 2 cm/cycle on average, and the number of cycles varies little with counting method. We counted ~300 laminae between 600 cm (13460 ka) and 1201 cm (14408 ka) where the deposition rate is uniformly high, and those reflect ~300 oscillations in terrigenous input to the continental slope that are probably not annual (300 laminae/948 years = 0.32 laminae/yr) unless the age model underestimates the rate of sedimentation. Note that the calendar ages give lower accumulation rates than those using conventional ¹⁴C years as in Fig. 2F.

519 typical looking magnetic susceptibility. Not knowing what was present, we began with
520 samples ~20 g dry every 50 cm. Based on early $\delta^{18}\text{O}_{\text{Nps}}$ results, sampling was increased
521 to every 10 cm. About 20 clean and clear (not infilled) specimens of Nps were chosen
522 for stable isotope measurements using standard methods⁵⁵. Although the focus of the
523 stable isotopes in this paper is $\delta^{18}\text{O}$, $\delta^{13}\text{C}$ was measured and is reported in **Table ED2**.
524 Note that the $\delta^{13}\text{C}$ data are featureless for both Nps and *C. neoteretis*. They compare well
525 with the $\delta^{13}\text{C}$ of dissolved inorganic carbon reported from the eastern Beaufort Sea⁵⁶.

526

527 **4. Chronology**

528 **4.1 Gulf of Mexico**

529 Leventer et al.⁵⁴ was the first study to improve on the original Kennett and
530 Shackleton⁴ $\delta^{18}\text{O}$ data with a new higher resolution series from piston core EN32 PC6 in
531 anoxic Orca Basin and with bulk organic ^{14}C dates. That was before AMS dating, so as
532 the interest in meltwater diversion and the origin of the YD grew in the 1980s, Broecker
533 et al.^{9, 57} used AMS methods to redate the core. Unfortunately, their results contained
534 substantial age reversals. We include Leventer et al.⁵⁴ data in Figure 5 because they
535 provide a Holocene context for the higher resolution and better dated $\delta^{18}\text{O}$ series of
536 Williams et al.⁵. The two data sets are in good agreement where they overlap. However,
537 this was achieved by (selective) use of the available AMS dates at 29.5, 436.5, 471.0,
538 486.5, and 809 cm (refs 9, 57) and calibration using $\Delta R=0$.

539

540

541 **4.2 Beaufort Sea**

542 Levels for AMS dating (at NOSAMS) were identified based on the $\delta^{18}\text{O}_{\text{Nps}}$
543 results, and resampled so that as much as 80 g dry were picked to get sufficient Nps.
544 Where possible, only clean specimens of Nps and *C. neoteretis* were selected from the
545 size fraction $>150\ \mu\text{m}$. This was easy for *C. neoteretis* because the test is transparent, but
546 for Nps we set aside clean and empty specimens and cleaned the remainder mechanically
547 as described elsewhere⁵⁸. If that did not clean them sufficiently, we cleaned them
548 ultrasonically, always setting aside clean ones at each step. Ultrasonic cleaning broke up
549 most tests, but clean fragments were sometimes selected for inclusion in the dated
550 sample. Our chronology is based on a Bayesian age model (Figure ED6) using the Nps
551 dated levels (**Table ED1, Fig. ED3**).

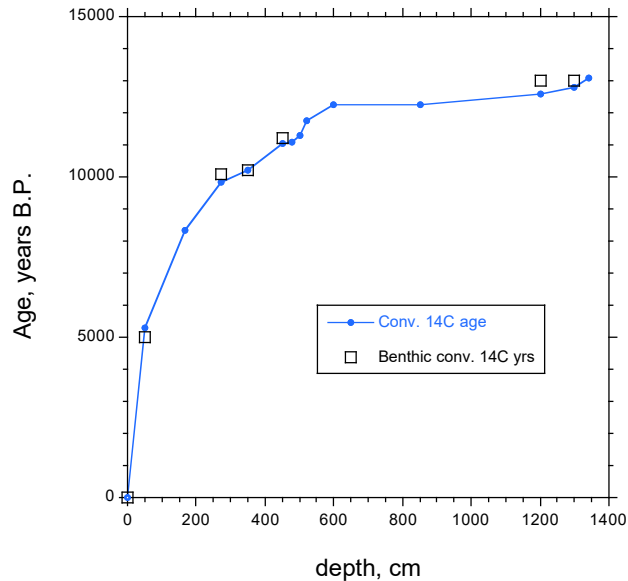


Fig. ED3. Age-depth relationship of conventional AMS ^{14}C dates on Nps (blue circles) and *C. neoteretis* (open black squares) from JPC-15.

552
 553
 554
 555
 556
 557
 558
 559
 560
 561
 562
 563
 564
 565
 566
 567
 568
 569

4.3 Choice of ΔR
A. Pre-bomb ΔR

Any discussion of ΔR should begin with the modern, or better yet, the pre-bomb ocean. For the Beaufort Sea, the pre-bomb ΔR has been estimated based on radionuclide tracers for Arctic processes^{30, 59} (Fig. 5), and in pre-bomb museum specimens of mollusks (especially bivalves⁶⁰). These are very different data sets and the resulting ΔR s are not directly comparable because the mollusk data came from specimens collected along the nearshore continental shelf whereas the ice station data (and our core sites) are far offshore. One notable thing about the Ostlund et al.³⁰ analysis is discussion of the ^{14}C measurement on surface waters in the east Greenland Current in 1957 that leads them to “safely assume” that shelf water had a pre-bomb $\Delta^{14}\text{C}$ of $-48 \pm 3 \%$. (These data were published first by Fonselius and Ostlund⁶¹ before international standardization.) Although east Greenland is about as far as you can get in the Arctic from the Beaufort Sea, Ostlund and Hut⁵⁹ showed that the residence time of shelf and near surface waters in the Arctic is only ~ 10 years. However, they had no shelf water data from the west Arctic where there



570
571

Fig. ED4. Locations of pre-bomb bivalve data⁶⁰ from off Alaska on left, downstream in the Amundsen Gulf (middle), and far to the east in Foxe Basin. These sites were chosen to define a flow path where Bering Strait water always hugs the coast and turns right. Today the shelfbreak current has been traced to the entrance of Amundsen Gulf³⁶, but the bivalve ¹⁴C data have a Pacific signature as far to the east as northern Foxe Basin.

572 is low “preformed” $\Delta^{14}\text{C}$ from the Pacific, based on the bivalves.
 573 McNeely et al.⁶⁰ compiled mollusk ¹⁴C data from all around Canada for the
 574 specific purpose of knowing ΔR at continental shelf depths. In the Beaufort-Chukchi
 575 Seas they reported dates on 7 bivalve specimens collected from two stations (**Fig. ED4**).
 576 Six bivalves were suspension feeders and one was a deposit feeder; that one is
 577 significantly older than the others ($\Delta R=610$ yrs). Excluding that datum, the others have a
 578 mean ΔR of 440 ± 101 yrs, or a mean $\Delta^{14}\text{C}$ close to -100 ‰. That result is greatly
 579 different than the $\Delta^{14}\text{C}$ of -48 ‰ directly measured in in East Greenland shelf waters³⁰.
 580 The missing element in the Ostlund and Hut⁵⁹ and Ostlund et al.³⁰ analysis was a
 581 source of relatively old waters from the NE Pacific via the Alaska Coastal Current and,
 582 through Bering Strait, to the shelf break current in the Beaufort Sea. The shelf break
 583 current can be traced as far east as Amundsen Gulf, by which point it is dissipated
 584 without evidence of entering the Gulf³⁶, but the pre-bomb mollusk data⁶⁰ can be used to
 585 trace transport to the Labrador Sea through the Canadian archipelago in recent times.
 586 Forty $\Delta^{14}\text{C}$ measurements of Pacific mollusks (Victoria, BC to Bering Strait), excluding
 587 deposit feeders, average $\Delta R=388 \pm 86$ yrs, not significantly different from the
 588 Chukchi/Beaufort value cited above (440 ± 101 yrs). By Amundsen Gulf, where

589 McNeely et al.⁶⁰ have 7 observations from 5 sites (Fig. ED4), the result, $\Delta R=350\pm 116$, is
590 within uncertainty of the Bering Strait source waters. However, by Foxe Basin, $\Delta R=286$
591 ± 74 yrs (n=8), significantly lower (younger) than the Beaufort/Bering Strait data. We
592 choose Foxe Basin as an end point because it represents a pathway that is least likely to
593 encounter younger Atlantic shelf waters, and for the same reason we only use those data
594 on the south side of the strait that connects Gulf of Boothia to Foxe Basin. Nevertheless,
595 a trend of increasing $\Delta^{14}\text{C}$ in pre-bomb mollusks from the Gulf of Alaska to Foxe Basin
596 suggests mixing with a young North Atlantic component. These data are substantially
597 older than the East Greenland mollusks, where $\Delta R=92 \pm 67$ years (n=12).

598 The east Greenland shelf is the only place where pre-bomb $\Delta^{14}\text{C}$ has been
599 measured in both shelf waters (-48 ± 3 ‰) and in mollusks (-61 ± 7 ‰), and with results in
600 reasonable agreement. However, this does not mean that shelf ΔR should be used to
601 calibrate ^{14}C ages from foraminifera on the Beaufort continental slope for a few reasons.
602 (1) The shelfbreak waters that carry the old signal from Bering Strait are well inshore of
603 the surface water overlying our core sites³⁶. (2) Although we do not know the pre-bomb
604 ^{14}C age of Beaufort Sea surface waters (Fig. 4), the rather close agreement of paired
605 benthic and planktonic ^{14}C ages suggests the planktonics live in water influenced by the
606 Atlantic layer even in the Holocene. During pre-Holocene time (>11 ka), before Bering
607 Strait was flooded^{26, 27}, the Atlantic layer might have shoaled in the absence of Pacific
608 water, all else being equal (pers. comm. 2016 from R. Pickart and M. Spall). However,
609 most importantly, (3) the absence of old Pacific water in the pre-Holocene Arctic means
610 that shelf waters must have had much lower ΔR than today prior to 11 or 12 ka.

611

612 B. ΔR in the Nordic Seas

613 There are no data from the western Arctic Ocean that can be used to estimate ΔR ,
614 so we turn to the Nordic Seas where waters feeding the Arctic surface circulation flow
615 northward along the coast of Norway, and southward from Fram Strait along the
616 Greenland coast to the Labrador Sea. The only useful data sets for this come from
617 Bondevik et al.²⁸ and Cao et al.²⁹. Cao et al.²⁹ synthesized existing ^{14}C data from the high
618 latitude North Atlantic and presented new data on solitary corals from Orphan Knoll
619 (1600 m water depth). They concluded that the Allerod warm period had a ΔR similar to
620 today (~ 0 years), and that ΔR was likely about 200 yrs greater during the YD. The
621 Bondevik et al.²⁸ data contributed greatly to that conclusion. Orphan Knoll data do not
622 reflect coastal conditions but rather the ventilation of the central Labrador Sea, with an
623 unknown transit time from the surface to ~ 1600 m.

624 Accordingly, we base our surface reservoir corrections for the eastern Beaufort
625 Sea on the Bondevik et al.²⁸ data for samples where pairs of marine and terrestrial
626 (atmospheric) ^{14}C dates came from within 1-cm of each other in their cores, and not
627 including data the authors rejected as coming from out-of-place fossils. The difference in
628 conventional ^{14}C age between the marine and terrestrial data is defined as ΔR , and
629 terrestrial dates have been recalibrated using Calib 7.1 using the Marine 2013 curve.

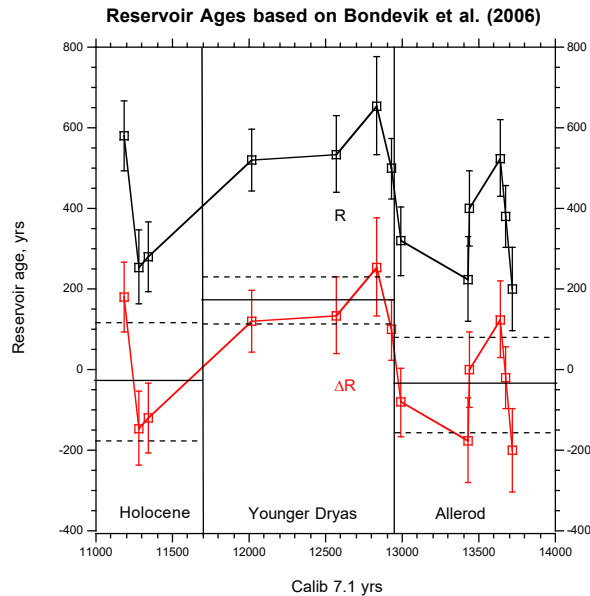


Fig. ED5. Summary of R and ΔR for the Allerod through the early Holocene based on pairs of marine and terrestrial ^{14}C dates from Bondevik et al.²⁸. Vertical error bars are $\pm 1\sigma$. Horizontal lines show mean values for the three time intervals, with dashed lines representing $\pm 1\sigma$.

630
631
632
633
634
635
636
637
638
639
640
641
642
643
644
645
646
647
648
649

For the Allerod there are seven marine-terrestrial pairs of AMS dates²⁸ that return a mean of -36 ± 116 years (1σ) (**Figure ED5**). For the Younger Dryas and Holocene, the statistics are 170 ± 60 ($n=3$) and -28 ± 148 ($n=3$), respectively. Although these data essentially come from only one location and are highly variable, they are the only dates that meet our requirement of being in the flow of coastal waters either entering or leaving the Nordic Seas. The low Allerod and higher YD ΔR are consistent with the synthesis of Cao et al.²⁹ and it makes sense that, during that relatively warm period with better North Atlantic ventilation, the reservoir effect would have been similar to the Holocene. The Holocene results are generally concordant with the pre-bomb estimate of Ostlund³⁰. For calibration purposes we chose $\Delta R = 0 \pm 100$ years for the Holocene and the Allerod, and 200 ± 100 for the YD. These values are increased somewhat from the measured values (Fig. ED5) because there is some evidence for increased ΔR with latitude along the Norwegian coast, but even the authors who made that observation do not agree about its significance⁶². Note that for dating the beginning of the YD it is important to use the Allerod ΔR , not that of the YD. This is because if the YD flood caused a decrease in the AMOC, and if that caused the increase in ΔR through changes in storage and exchange in the ocean-atmosphere carbon system, then the Allerod ΔR is more appropriate than the YD ΔR .

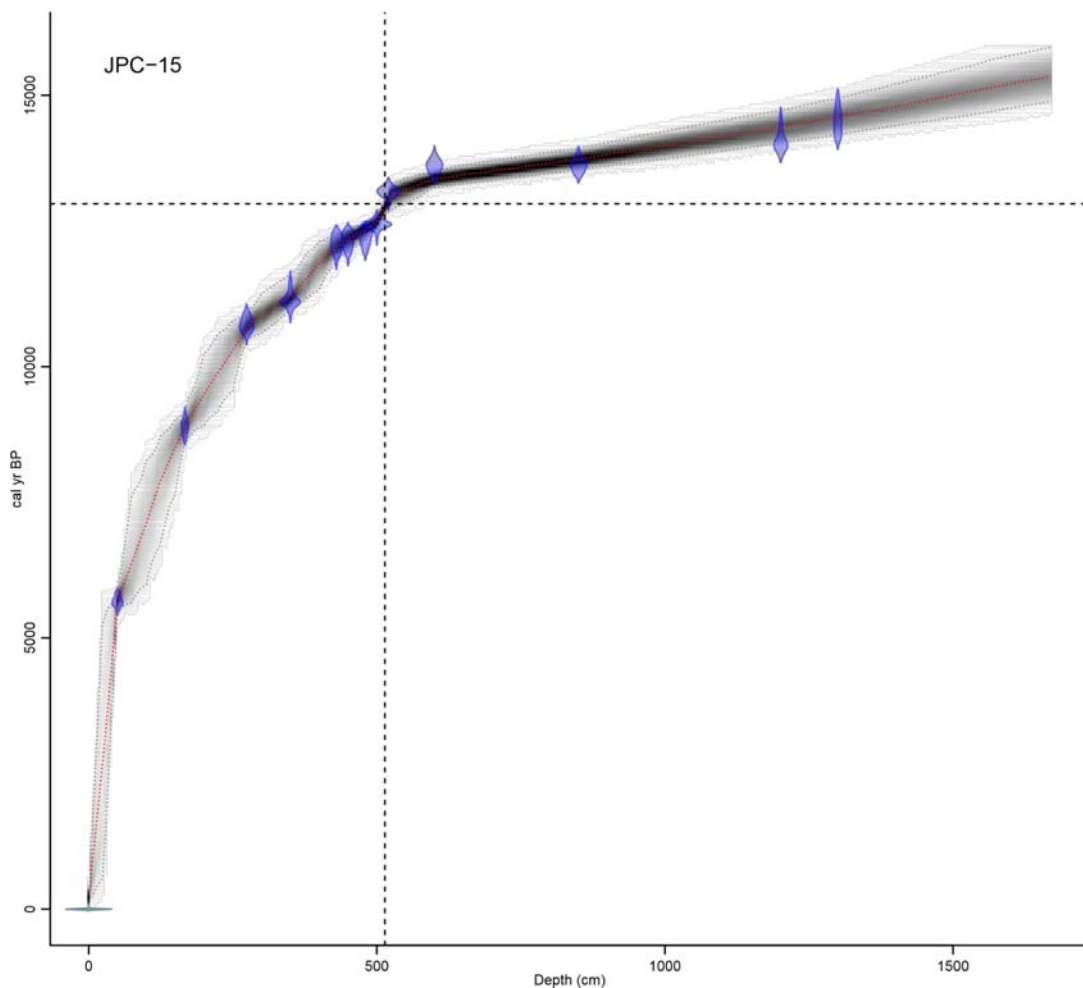
650 4.4 Bayesian age modeling.

651
652
653
654
655
656
657
658
659

As recommended by an anonymous reviewer, we developed an age model for JPC15/27 using the “Bacon” software of Blaauw and Christen⁶³ (2011). This method evaluates rates of sedimentation for discrete sections of the core, and these are informed by results in surrounding sections. The appropriate command settings for our model are: Bacon(“JPC-15”, 25, acc.mean=2, acc.shape=1.1, normal=TRUE, remember=FALSE, depths.file=T), agedepth(rotate.axes=TRUE, rev.yr=TRUE). We input our ^{14}C dates with the higher ΔR during the YD, we fixed the core top to equal zero years, and the calibration was done using the Marine 13 curve. The resulting age-depth relationship (**Fig. ED6**), illustrates the mean age of levels in the core and the 95% confidence interval.

660 Of critical importance is the calendar age of the sample at 514 cm, where $\delta^{18}\text{O}$ is about
661 halfway to its minimum value: 12,939 calendar years B.P., with a minimum age of
662 12,786 years and a maximum age of 13,080 years, or about 12.94 ± 0.15 ka. The abrupt
663 decrease in $\delta^{18}\text{O}$ lies within the 95% confidence interval of 13 ka, the nominal date for
664 the diversion of meltwater from the Gulf of Mexico⁵, and before the $\sim 12,850$ year start of
665 the YD on the Greenland ice core timescale³⁴.

666 We experimented with other age models, to test the robustness of our result.
667 Using a constant ΔR of 0 ± 100 yrs for the entire record gave about the same age for the
668 sample at 514 cm with the variable ΔR model, so we know that the “bacon” age is not
669 influenced by the decrease of sedimentation rate and increase in ΔR during the YD.
670 Likewise, doubling the uncertainty in ΔR for the entire record returns the same ages but
671 with less confidence. In sum, our conclusions are driven mostly by the choice of ΔR ; we
672 cannot reject the hypothesis that the flood down Mackenzie River was coincident with
673 the beginning of the Younger Dryas cooling using any DR that is consistent with the
674 Allerod data (Fig. ED5). Using our preferred age model (Fig. ED6), we summarize ages
675 and uncertainties associated with the $\delta^{18}\text{O}_{\text{Nps}}$ evidence for the YD flood in JPC15/27 in
676 **Table ED3**.
677



678

Figure ED6. Age model for JPC15/27 using the Bayesian method “Bacon”⁶³. Horizontal dashed line is at 13 ka and vertical dashed line is at 514 cm. The model gives an age at 514 cm of 12.94 ± 0.15 ka. A blow-up of the critical $\delta^{18}\text{O}_{\text{Nps}}$ data 12-13.5 ka is shown in Figure ED7.

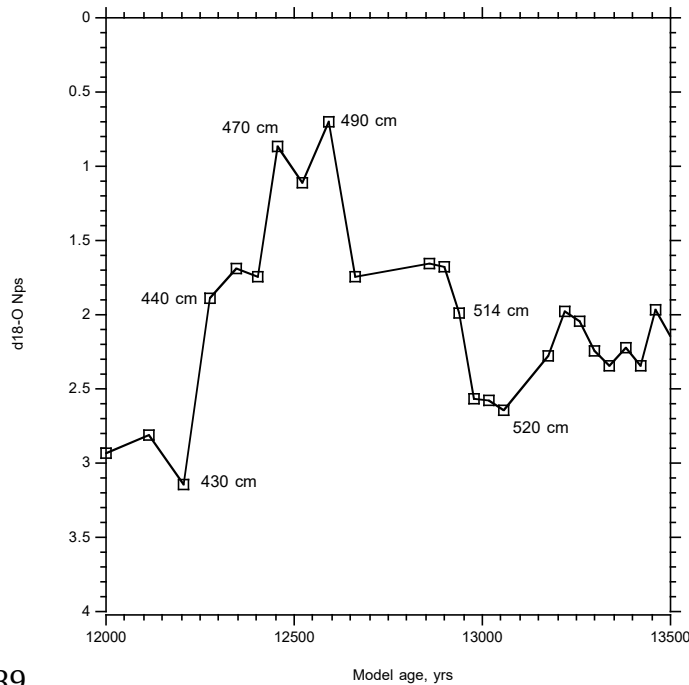
679

680

681 5. Regional summary of oxygen isotope data

682 5.1 New core data from this study

683 It is important to determine the spatial extent of the YD flood within the Beaufort
 684 Sea because Coriolis forcing would drive a buoyant flow to the right from Mackenzie
 685 River, and northward along the Canadian Archipelago toward Fram Strait. Such a direct
 686 path to the North Atlantic might have the most climate impact because the surface waters
 687 would be freshest. On the other hand, wind forcing could counteract the Coriolis driven
 688



ED Fig. 7. Blow-up of $\delta^{18}\text{O}_{\text{Nps}}$ data associated with the YD flood at JPC15/27. The depth of important features is indicated for reference to ED Table 3. We interpret these data to mean that the flood was underway as early as 12940 ± 150 years ago, the age of the sample at 514 cm.

689
690

691 flow and perhaps allow more mixing with Beaufort Gyre. In that case, the freshening in
692 the North Atlantic region might have been less but may have lasted longer.

693
694
695
696
697
698
699
700
701
702
703

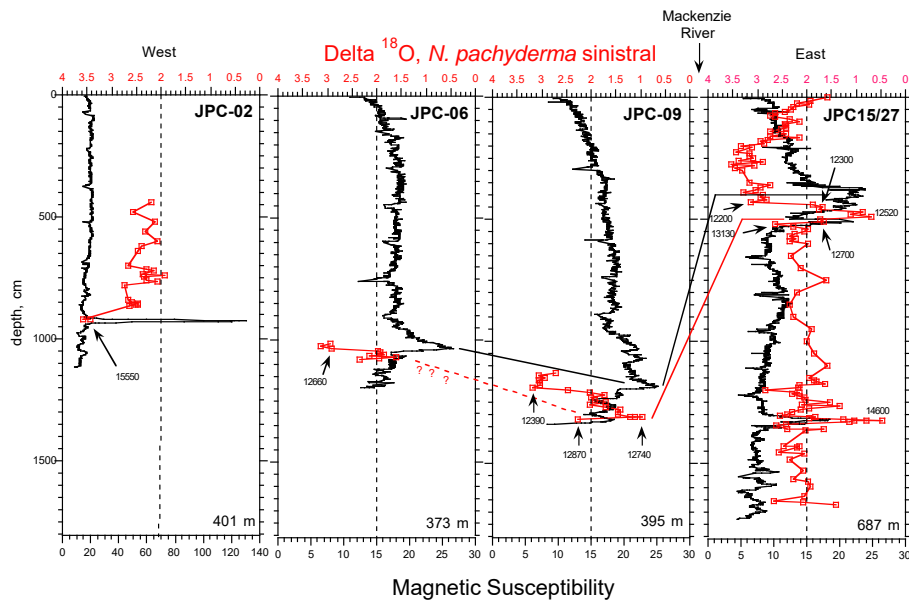
Here we summarize the stratigraphic data from cores extending from JPC15/27 in the east, which we consider to be a “type section,” to other cores as far west as Barrow, AK (Fig. ED8). West of Mackenzie River at JPC-09 we have identified a $\delta^{18}\text{O}_{\text{Nps}}$ minimum at about 13 m below the seafloor. It reaches 1 ‰, close to the minimum at JPC15/27 and it occurs a meter below a prominent maximum in magnetic susceptibility. This phasing is similar to results at JPC15/27, and the AMS date at JPC-09 falls within the range of dates constraining the flood event to the east. The brief peak in magnetic susceptibility at JPC15/27 at ~500 cm is not matched at JPC-09 probably because the ice rafting, which becomes common >1300 cm, stopped the corer. If we calibrate the YD ¹⁴C ages from JPC-09 (Table ED1) with $\Delta R=200\pm 100$, the $\delta^{18}\text{O}_{\text{Nps}}$ changes are well-matched at the two cores (Fig. 5, Fig. ED9).

704
705
706
707
708
709
710

JPC-09 is very close to core P45 of Andrews and Dunhill (2004)(Fig. 1), so we recalibrated the age model for that core using $\Delta R= 0\pm 100$ (post YD) and plotted their $\delta^{18}\text{O}_{\text{Nps}}$ with the new data from this study (Fig. ED9). The agreement between these cores is good, although the age model may make the bottom of P45 too old because their oldest date was on benthic foraminifera. Note that the minimum in $\delta^{18}\text{O}_{\text{Nps}}$ was not found by Andrews and Dunhill (2004), most likely because the corer failed to penetrate the ice rafted layer at about 5 m subbottom.

711
712
713
714
715

Continuing farther west of Mackenzie River, the $\delta^{18}\text{O}_{\text{Nps}}$ at JPC-06 records only a small minimum before the main peak in magnetic susceptibility (Fig. ED8). This suggests that the YD meltwater plume must have been very localized to the region east of this site with only minor salinity lowering of the near surface ocean. Of the samples examined, a small peak in ice rafting is associated with the small minimum in $\delta^{18}\text{O}_{\text{Nps}}$.



716
717

Figure ED8. Comparison of magnetic susceptibility and $\delta^{18}\text{O}_{\text{Nps}}$ stratigraphies in a zonal transect of cores from east of Mackenzie River (JPC15/27) to Barrow, AK (JPC-02). The vertical dashed line in each core marks the baseline $\delta^{18}\text{O}_{\text{Nps}}$ as reference for surface freshening. The solid black and red lines correlate the magnetic susceptibility $\delta^{18}\text{O}_{\text{Nps}}$ peaks, respectively. Note the decreasing influence of $\delta^{18}\text{O}_{\text{Nps}}$ lowering (freshening) from east to west.

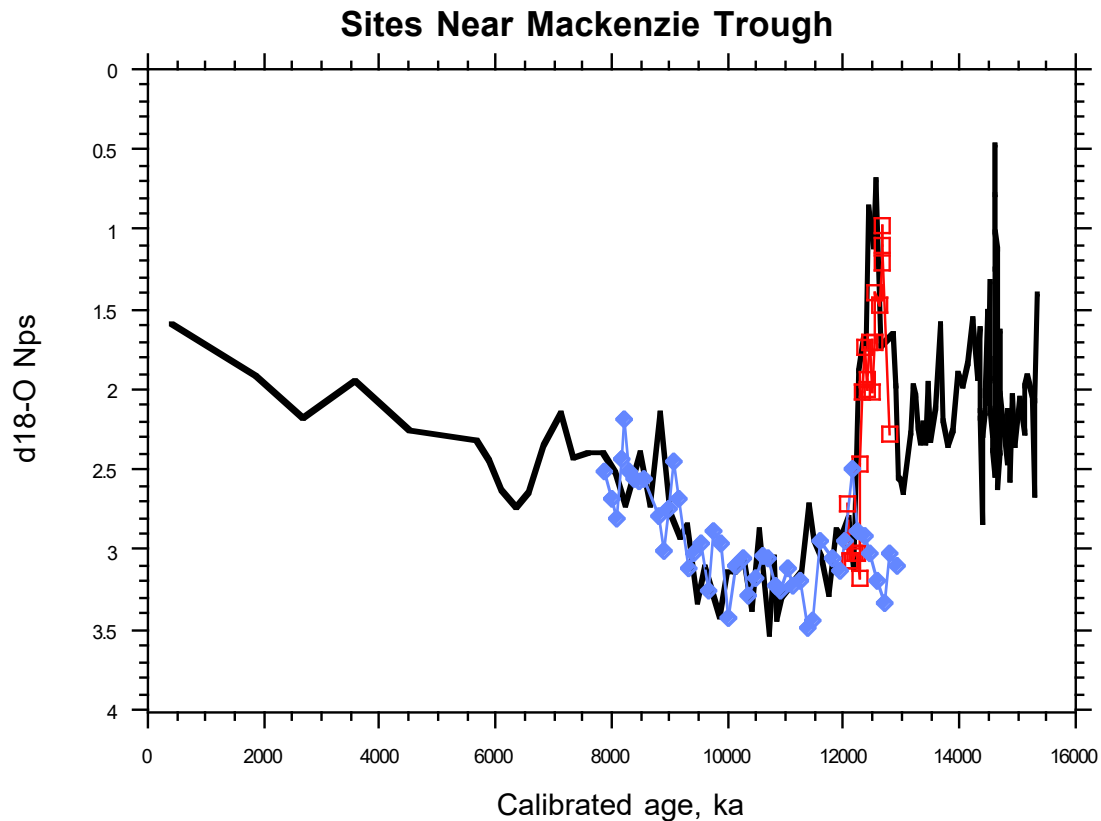
718

719 In the Chukchi Sea off Barrow, AK, the most notable feature of JPC-02 is an IRD
720 and magnetic susceptibility peak at ~920 cm that dates to 15.55 calibrated ka and
721 includes a 6-cm dark non-carbonate dropstone. Because this event is not recorded far to
722 the east at JPC15/27, and is >1000 years older than the 14.6 ka event at that site, it gives
723 a maximum age for the bottom of the composite section at JPC15/27, assuming the event
724 came from the Canadian Archipelago and would probably have spread across the
725 Beaufort Sea. That maximum age (15.5 ka) agrees well with the 15.4 ka extrapolated age
726 for the end of the JPC15/27 $\delta^{18}\text{O}_{\text{Nps}}$. Also of note is the maximum in $\delta^{18}\text{O}_{\text{Nps}}$ coincident
727 with this IRD layer; this is the opposite of what we see in the YD and 14.6 ka events
728 closer to Mackenzie River and it is the heaviest we have measured in this study.

729

730 Most of the $\delta^{18}\text{O}_{\text{Nps}}$ data fall higher than the 2 ‰ reference level for the entire
731 record <15.5 ka (Fig. ED8), similar to the nearby Holocene results from Keigwin et al.²⁶.
732 Thus, taking into account the ice volume effect on $\delta^{18}\text{O}$, we conclude that the near sea
733 surface off Barrow was fresher than today during most of the deglaciation, but there must
734 also have been a salinity gradient from the Chukchi Sea to the eastern Beaufort Sea. This
735 points to Mackenzie River as the source of the freshening, but the absence of evidence for
736 the YD flood off Barrow suggests that floodwaters were not diluted much by mixing in
the Beaufort Gyre. If supported by further data, this could mean that the YD flood was

737 brief compared to the mixing time of the Beaufort Gyre and might have been especially
738 potent in affecting the AMOC.
739



740

Fig. ED9. Comparison of $\delta^{18}\text{O}_{\text{Nps}}$ data between JPC15/27 (black line), JPC-09 (red squares) and core P45 (blue diamonds)⁶⁴. Note the excellent agreement of minima in $\delta^{18}\text{O}_{\text{Nps}}$ from this study.

741

742 5.2 Other published core data

743 Several papers report stable isotope and radiocarbon data from the western Arctic
744 (Mendeleyev Ridge) including, for example, Poore et al.⁶⁵ and Polyak et al.⁶⁶. We cannot
745 directly correlate our results from the eastern Beaufort Sea with those because they have
746 much lower rates of sedimentation and fewer ¹⁴C dates. Given that we also cannot
747 correlate to our own core off Barrow (**Fig. ED8**), which does have high rates, it is
748 possible that there was substantial spatial variability in near surface ocean conditions in
749 the western Arctic during deglaciation. As an example of this, both Poore et al.⁶⁵ and
750 Polyak et al.⁶⁶ found deglacial minima in $\delta^{18}\text{O}_{\text{Nps}}$ that are 0 ‰ or even lower. These are
751 probably not evidence of the YD flood from Mackenzie River because the $\delta^{18}\text{O}_{\text{Nps}}$ is
752 lower than we observe closer to the source, and the rates of sedimentation are probably
753 too low to resolve such a brief event.

754 Closer to the Beaufort Sea, on the Chukchi Borderlands, Polyak et al.⁶⁷ do find a
755 $\delta^{18}\text{O}_{\text{Nps}}$ minimum of about 1 ‰ that could be related to one of those we see at core 15/27.

756 However, using $\Delta R=0$, their benthic foram calibrated date for that event is 13.8 ka which
757 falls between the events we have found. That event is associated with a small peak in ice
758 rafting (but not magnetic susceptibility), and below that there is a much larger undated
759 IRD event coincident with a large peak in magnetic susceptibility.

760 In addition to the comparisons discussed above, we can also correlate to results
761 from Mackenzie Trough near our JPC-13 (ref. 41). One of their cores sampled the same
762 high $\delta^{18}\text{O}_{\text{Nps}}$ (3.11 ± 0.28 ‰, $n=9$) interval ~ 10 -12 ka as in JPC15/27. The Schell et al.⁴¹
763 data fall mostly between 10.9 and 10.6 ka when recalibrated.

764

765 **Extended Data references:**

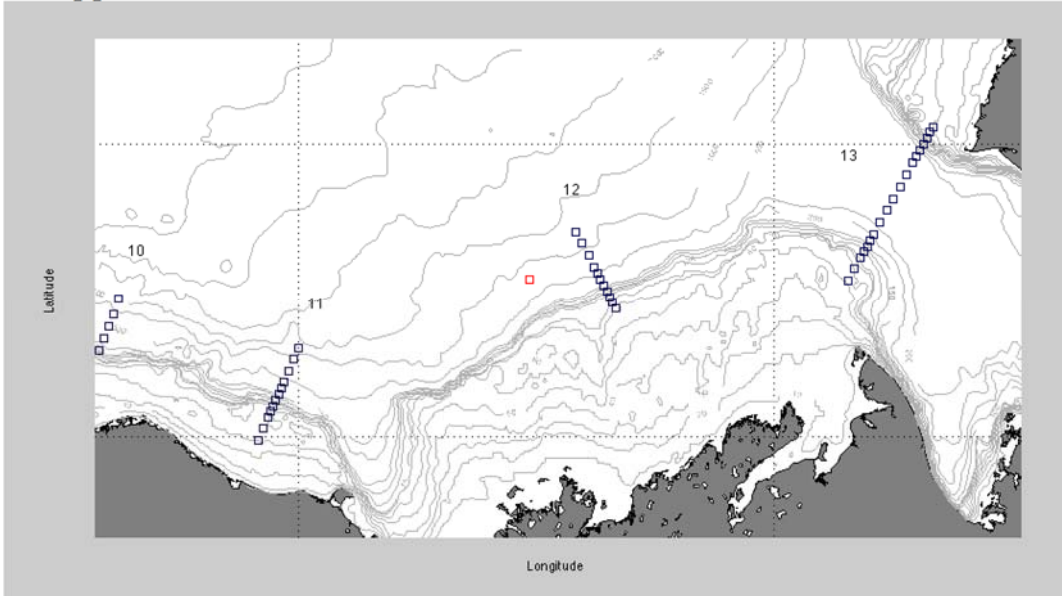
766

- 767 55. Keigwin, L.D. Radiocarbon and stable isotope constraints on last glacial maximum
768 and Younger Dryas ventilation in the western North Atlantic. *Paleoceanography*
769 **19**, doi: 10.1029/2004PA001029 (2004).
- 770 56. Oxtoby, L.E., Mathis, J.T., Juranek, L. W. & Wooller, M. .J. Estimating stable carbon
771 isotope values of microphytobenthos in the Arctic for application to food web
772 studies. *Polar Biol.* **39**, 473-483 (2016).
- 773 57. Broecker, W.S. et al. Accelerator mass spectrometric radiocarbon measurements on
774 foraminifera shells from deep sea cores. *Radiocarbon* **32**, 119-133 (1990).
- 775 58. Keigwin, L.D. & Lehman, S.J. Radiocarbon evidence for a benthic front near 3.1 km
776 in the Equatorial Pacific Ocean. *Earth Planet. Sci. Lett.* doi:
777 [/10.1016/j.epsl.2015.05.025](https://doi.org/10.1016/j.epsl.2015.05.025) (2015).
- 778 59. Ostlund, H. G. & Hut, G. Arctic Ocean water mass balance from isotope data. *Jour.*
779 *Geophys. Research* **89**, 6373-6381 (1984).
- 780 60. McNeely, R., Dyke, A. S. & Southon, J. Canadian marine reservoir ages preliminary
781 data assessment. *Geological Survey of Canada open file 5049*: DOI:
782 10.13140/13142.13141.11461.16649 (2006).
- 783 61. Fonselius, S. & Ostlund, G. Natural radiocarbon measurements on surface water from
784 the North Atlantic and the Arctic Sea. *Tellus* **11**, 77-82 (1959).
- 785 62. Mangerud, J. Bondevik, S., Gulliksen, S., Hufthammer, A.K. & Hoisaeter, T. Marine
786 ^{14}C reservoir ages for 19th century whales and molluscs from the North Atlantic.
787 *Quaternary Science Reviews* **25**, 3228-3245 (2006).
- 788 63. Blaauw, M. & Christen, J. A. Flexible paleoclimate age-depth models using an
789 autoregressive gamma process *Bayesian Analysis* **6**, 457-474 (2011).
- 790 64. Andrews, J. T. & Dunhill, G. Early to mid-Holocene Atlantic water influx and
791 deglacial meltwater events, Beaufort Sea slope, Arctic Ocean. *Quaternary Res.*
792 **61**, 14-21 (2004).
- 793 65. Poore, R. Z., Osterman, L., Curry, W. B. & Phillips, R. L. Late Pleistocene and
794 Holocene meltwater events in the western Arctic Ocean. *Geology* **27**, 759-762
795 (1999).
- 796 66. Polyak, L., Curry, W. B., Darby, D.A., Bischof, J. & Cronin, T. M. Contrasting
797 glacial/interglacial regimes in the western Arctic Ocean as exemplified by a
798 sedimentary record from the Mendeleev Ridge. *Palaeogeog., Palaeoclim.,*
799 *Palaeoeco.* **203**, 73-93 (2004).

800 67. Polyak, L., Darby, D. A., Bischof, J. F., & Jakobsson, M. Stratigraphic constraints on
801 late Pleistocene glacial erosion and deglaciation of the Chukchi margin, Arctic
802 Ocean. *Quat. Res.* **67**, 234-245 (2007).

803
804
805
806

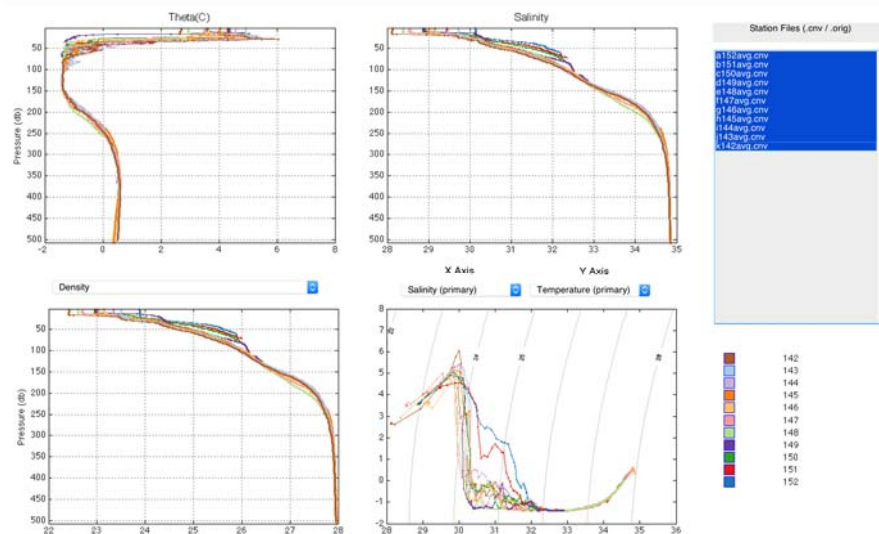
ED Appendix 1.



807
808

ED Appendix Fig. 1. HLY1003 Station positions for the hydrographic data in ED Appendix Fig. 2 provided by Dr. Robert Pickart (WHOI). The position of HLY core JPC15/27 is shown as a red square.

809



810

811

ED Appendix Fig. 2. Data for section 12 presented vs pressure (~depth) as potential temperature (upper left), salinity (upper right), density (lower left), and T vs S (lower right). All hydrographic data are available at: <http://aon.who.edu>. 812